Challenge Journal of Concrete Research Letters

Research Article

Fracture properties of self-compacting fiber-reinforced concrete

Mariam Farouk Ghazy [a,*], Metwally Abd Allah Abd Elaty [a], Omar Daboun [b]

[a] *Department of Structural Engineering, Tanta University, PC 31733 Tanta, Egypt*

[b] *Department of Civil Engineering, Delta Higher Institute for Engineering and Technology, Mansoura, Egypt*

ABSTRACT

Self-compacting concrete (SCC) is an innovative concrete that does not necessitate vibration for placing and compaction. Nineteen concrete mixes were investigated including a control mix without fibers as well as eighteen SCC with fibers (SCFRC) mixes. Three types of fibers (polypropylene, glass and steel) were used. Slump flow, L-box, V-funnel as well as column segregation tests were conducted to assess the fresh properties. Whereas, compressive, splitting tensile and flexural strengths were measured to assess the hardened properties of SCFRC. Three point bending tests were performed for the purpose of assessing the fracture properties of SCFRC. Test results showed that the inclusion of fibers to produce SCFRC mixtures remarkably enhanced the fracture properties including fracture energy (G_f) and fracture toughness (K_{1c}). Inclusion of steel fibers with 2% volume fractions showed an improvement with 26.9 times for G_f over the control mix. Whereas, 104% increase in K_{1c} was recorded for the same mix over the mix without fibers. Adding fibers to SCC to produce self-compacting fiber reinforced concrete (SCFRC) will expand its advantages. However, the application fields still need to understand the properties of SCFRC.

ARTICLE INFO

Article history:
Received 10 July 2020
Revised 11 October 2020
Accepted 19 November 2020

Keywords:
Self-compacting concrete
Fiber-reinforced concrete
Fresh properties
Fracture properties

1. Introduction

The Japanese researchers and engineers took the responsibility of developing a special kind of concrete that can be placed and finished with less skilled laborers. Consequently, the notion of Self-compacting concrete (SCC) was first generated in Japan in 1986 (Douglas, 2004). SCC is an innovative concrete that does not necessitate vibration for placing and compaction. It is fully filling formwork and attaining full compaction under its own weight without the requirement, of any type of compacting or external vibration. High segregation resistance, great passing ability and exceptional ability to flow around obstacles, congested steel reinforcement and tight sections are the three main advantages of SCC (Okamura and Ozawa, 1995). SCC also has another major benefit compared to traditional concrete, it is used to minimize the noise level in construction sites and decrease the impact on the environment (Persson, 2001). In addition to accelerate the rate of concrete casting, diminishing construction times, improving the quality of concrete and reducing the overall cost are also benefit of its implementation.

Adding fibers to SCC to produce self-compacting fiber-reinforced concrete (SCFRC) will expand its advantages. Fibers bridge cracks and restrict its ingeneration and therefore enhance flexural and tensile strengths (Groth and Nemegeer, 1999; Khayat and Roussel, 1999; Alberti et al., 2014a; Ghazy et al., 2015; Hoang and Fehling, 2017; Adhikary et al., 2019).

Fracture mechanics is the field of solid mechanics involved in the study of the expansion of cracks in materials and the quantitative relations between the crack length, the material's deep-rooted resistance to crack growth, and the stress at which the crack expands at high speed to cause structural failure. The crack path through a composite material such as concrete is dependent on the mechanical interaction between the aggregates and the binder matrix. Fracture energy (G_f) of a composite material which is defined as the amount of energy necessary to create one-unit area of a crack (Barros and Figueiras, 1999). The result of G_f depends on the deviation of the

* *Corresponding author*. Tel.: +2-040-345-0532 ; Fax: +2-040-345-3860 ; E-mail address: mariam.ghazy@f-eng.tanta.edu.eg (M. F. Ghazy)
ISSN: 2548-0928 / DOI: https://doi.org/10.20528/cjcrl.2020.04.004

crack path from an idealized crack plane (Sabir et al., 1997; Wittmann, 2002). The value of fracture toughness (K_{1c}) indicates the magnitude of the stress concentration in front of the crack tip when the crack starts to propagate.

Tension stiffening is the ability of concrete to carry tension between cracks, which provides additional stiffness for a RC member in tension before the reinforcement yields. It can significantly affect member rigidity, deflection, and width of cracks under service loads. The presence of steel fibers is effective in controlling splitting cracks and significantly increases the tension stiffening effect because SFRC can carry tensile stress through the crack (Morelli et al., 2017; Kytinou et al., 2020).

Adding steel or/and polypropylene fibers ranging from 0.25% to 1% showed that fiber bridges cracked on the fracture surface during the loading and delayed cracking, thus the element did not break as well as an extended post-peak softening behavior did occur. The shape of the descending branch was dependent on geometrical properties, mechanical properties and the quantity of the used fibers (Ghazy et al., 2015; Smarzewski and Barnat-Hunek, 2015).

Addition of low, medium and high fiber contents of macro polyolefin fibers to SCC was showed that the G_f obtained for all the polyolefin SCFRC mixtures is significantly higher when compared with the plain SCC. K_{1c} and ductility improvements are quite reliable even for the medium polyolefin fiber content mixtures based on Alberti et al. (2014b).

Biswajit and Mohanty (2015) added steel fibers to SCC then investigated the fracture properties of the produced SCFRC. The relationships between load and crack mouth opening displacement (CMOD) diagrams for SCFRC showed an increase in fracture energy properties of the SCFRC mixes owing to crack arresting mechanism of the fibers in the matrix. They concluded that the mixes including 0.2% and 0.25% steel fiber by weight of concrete exhibited best performance.

An experimental study to investigate fracture behavior of hybrid steel SCFRC was performed by Akcay and Tasdemir (2012). Three different types of steel fibers with and/or without hooked-ends were added to the mixtures in two different volume fractions (0.75% and 1.5% of the total volume of concrete). Based on their G_f test results, the mixes with high strength steel fibers exhibited behavior of enhanced toughness and ductility when compared to the concretes with normal strength steel fibers.

Different ratios of the notch depth to beam depth were used in fracture test specimens, Elices and Planas (1996) conducted an analysis of test results for different notch to beam's depth ratios and showed that a ratio of 0.2–0.5 can be considered as a practical experimental range. A ratio of 0.375 was used in the specimens of that study to make the ligament area sizable in order to enable the observation of the crack propagation in the concrete. Three or four-point bending tests on notched beams were usually carried out to evaluate the material fracture energy. The three-point bending tests on center-notched beams are more suitable to characterize the fracture parameters of SFRC (Hordijk, 1991).

From the above previous studies, the application fields still need to understand the properties of SCFRC. The main target of this study is to determine the fracture parameters of SCFRC after inclusion of different types and volume fractions of fiber and to make comparisons with SCC without fibers. For this purpose, load–deflection curves, G_f, K_{1c} and CMOD were calculated and assessed to investigate the fracture properties from three point bending tests on SCFRC notched beams.

2. Experimental Program

2.1. Materials

Natural siliceous sand with a specific gravity of 2.55 and a fineness modulus of 2.46 was used. The coarse aggregate used was crushed dolomite, with a specific gravity of 2.6. The crushing modulus was 23%, and the maximum nominal size was 10 mm.

The cement used was Portland cement (CEM I 42.5N) according to (ESS 4756-1-13), and (EN 197-1-11). Tap water free from impurities was used for mixing and curing the test specimens. Silica fume (SF) with specific gravity of 2.21 and specific surface area of 150000 cm^2/g was used and Class (F) fly ash (FA) meeting the requirements of ASTM C618-19 with a specific gravity of 2.1 was used.

High range water reducer admixture (HRWR) was used. The admixture is a brown liquid having density of approximately 1.080 kg/L at room temperature. The admixture permissible percentage is 1-3% of cement weight according to the manufacturer which is the polycarboxylic ether based and meeting the standard requirements of ASTM C494/C494M-19 (type F and G).

Three types of fibers, mainly, polypropylene (PP), glass (G) and steel (S) (straight fibers) were used. For PP fibers, two different shapes were used including straight and mesh. Moreover, two different aspect ratios of PP were conducted. The properties of the investigated fibers according to the manufacturer are presented in Table 1.

Table 1. Properties of the investigated fibers.

Type / shape		Length (L) (mm)	Diameter (d) (mm)	L/d	Modulus of elasticity (GPa)	Tensile strength (MPa)
Polypropylene fibers (PP)	Micro straight fibers (PM)	6	0.018	333	9	500
	Long straight fibers (PL)	18	0.018	1000		
	Micro fiber mesh (PF)	6	0.018	333		
	Long fiber mesh (PFL)	18	0.018	1000		
Glass fibers (G)		18	0.018	1000	72	1700
Steel fibers (straight) (S)		15	1	15	210	1250

2.2. Mix proportional

Nineteen concrete mixes were investigated including a control SCC mix without fibers as well as eighteen SCFRC mixes. The used fiber volume fractions were 0.25%, 0.5% and 0.75% by volume of concrete for the conducted PP fibers. Whereas, 0.15%, 0.25% and 0.4% volume fraction for G fibers were investigated. On the other hand, 0.5%, 1.0% and 2.0% volume fraction for S fibers were included. The net water to cementitious materials ratio (w/cm) for this study was varying from 27% to 39% and HRWR dosage used ranged from 1.5% to 2% (by weight of total cementitious materials) depending on fiber type and volume fraction. Concretes were produced by using SF and FA with percentages of 10% and 20% by weight of total cementitious materials, respectively. The concrete mix proportions for all mixes are detailed in Table 2.

Table 2. Concrete mix proportions, kg/m^3.

Fiber Type	Mix ID	F%	w/cm	C	FA	SF	Dolomite	Sand	Water	HRWR
Without fibers	SCC-0	0	0.27	420	120	60	700	700	162	9
Polypropylene micro fibers (PM), 6 mm	SCC-PM0.25	0.25	0.29	420	120	60	700	700	174	9
	SCC-PM0.5	0.5	0.31	420	120	60	700	700	186	12
	SCC-PM0.75	0.75	0.32	420	120	60	700	700	192	12
Polypropylene Long fibers (PL), 18 mm	SCC-PL0.25	0.25	0.29	420	120	60	700	700	174	9
	SCC-PL0.5	0.5	0.3	420	120	60	700	700	180	10.5
	SCC-PL0.75	0.75	0.38	420	120	60	700	700	228	12
Polypropylene micro fiber mesh (PF), 6 mm	SCC-PF0.25	0.25	0.29	420	120	60	700	700	174	9
	SCC-PF0.5	0.5	0.29	420	120	60	700	700	174	9
	SCC-PF0.75	0.75	0.3	420	120	60	700	700	180	10.5
Polypropylene long fiber mesh (PFL), 18 mm	SCC-PFL0.25	0.25	0.29	420	120	60	700	700	174	9
	SCC-PFL0.5	0.5	0.29	420	120	60	700	700	174	9
	SCC-PFL0.75	0.75	0.31	420	120	60	700	700	186	12
Glass fibers (G), 18 mm	SCC-G0.15	0.15	0.31	420	120	60	700	700	186	10.5
	SCC-G0.25	0.25	0.36	420	120	60	700	700	210	12
	SCC-G0.4	0.4	0.39	420	120	60	700	700	234	12
Steel fibers (S), 15 mm	SCC-S0.5	0.5	0.29	420	120	60	700	700	174	9
	SCC-S1	1	0.29	420	120	60	700	700	174	9
	SCC-S2	2	0.29	420	120	60	700	700	174	9

Note: F: Fibers, C: Cement, FA: Fly ash, SF: Silica fume

2.3. Specimen preparation

The dry materials required for each mix were weighted and mixed using a drum concrete mixer with 100 L total capacity. The water in addition to admixture and cementitious materials were mixed for a half minute to ensure the uniformity of the constituents. Sand was simultaneously charged into the mixer and was mixed for a half minute and then coarse aggregate was added and continue mixing for at least two minutes, finally fiber was added and then the mix was mixed for another 5 minutes.

The conducted specimens in this study for fracture test were 100 mm breadth (b), 80 mm depth (d) and 250 mm long (L) with a 30 mm notch (a) in the middle of the beam. Cubes with 100 mm side length were used for determining compressive strength. Whereas, cylinders with 100 mm diameter and 200 mm length were used for determining splitting tensile strength. On the other hand, prism specimens with a square section of the 100 mm side length and 500 mm total length were used to determine the flexural strength.

The concrete was placed in the steel molds without any compacting or vibrating, finally surfaces were finished using towel. All of the specimens were kept in their molds for 24 h after casting in moisture room at 25°C and 50% relative humidity, then they were removed from the molds and remarked with ID's then immerged in clean water at 20°C until the day of testing. All of specimens which tested after 56 days were taken out from the water after 28 days and kept in moisture room at 25°C and 50% relative humidity.

2.4. Testing procedures

Slump flow, L-box, V-funnel according to EFNARC-05 and Egyptian Technical Specification for Self Compacting Concrete (ESS 360-08) as well as column segregation tests according to ASTM C1610-19 were used to evaluate the consistency and workability of the fresh mixes of SCFRC. The slump flow test characterizes the flowability of the SCC, the V-funnel gives an indication of the viscosity and the increase of resistance to flow caused by the fibers, the L-box with reinforcement bars gives an indication of

passing ability through reinforcement, while the column segregation test evaluates stability of SCC against segregation. On the other hand, compressive strength, splitting tensile strength as well as flexural strength, were measured to assess the hardened properties of SCFRC.

Three point bending tests were performed by Universal Testing Machine (300 kN) for the purpose of assess the fracture properties of SCFRC. The ends of the specimens were placed on the supporting rollers at a span of 200 mm with the notch on tension side. Depth to notch ratio of 0.375 was used in the specimens of this study in line with Elices and Planas (1996) in order to enable the observation of the crack propagation in the concrete. Digital data acquisition system was incorporated with a load cell to record the load with an accuracy of 0.001 kN. The vertical displacement was measured by LVDT with an accuracy of 0.001 mm and 30 mm total capacity. The CMOD was measured by using Pie-shape (PI-5-100) fixed at the beam side. The Pie-shape was 100 mm gauge length, ± 5 mm capacity, 350Ω resistance and allowable bridge excitation of 10V. The data acquisition system had the ability to record up to 1000 data per second. A loading rate of 0.1 mm/min was used in the tests of this study. A high rate of data scanning per second was used to capture the post-peak part of the load–deflection curve. The load–deflection data were plotted to calculate the area under the curve.

The fracture energy (G_f) is the amount of energy necessary to create a crack on unit surface area projected in a plane parallel to the direction of propagation of crack, it is calculated from the work of fracture by using Eq. (1) according to RILEM TC 50–FMC.

$$G_f = \frac{W_0 + mg\delta_0}{A_{lig}} \quad (1)$$

where W_0 is the area under load deflection curve (N.m); mg is the self-weight of the specimen between supports (N), δ_{max} is the maximum displacement (m), A_{lig} is [b (d-a)] (m^2), b is the breadth of beam (m), d is the depth of beam (m), and a is the depth of notch.

K_{1c} is used to indicate the magnitude of the stress concentration that exists in front of the crack tip when the crack starts to propagate, Eq. (2) has been used in this study to calculate the K_{1c} (Bazant and Pfeiffer, 1987).

$$K_{1c} = \frac{3PL}{2bd^2} \times \sqrt{\pi a} \times \left[\frac{(1-2.5\,(A)+4.49(A^2)-3.98(A^3)+1.33(A^4)}{(1-A)^{3/2}}\right] \quad (2)$$

where P is the load (kN), A is a/d, L is the span of beam (m), b is the breadth of beam (m), d is the depth of beam (m), and a is the depth of notch (m).

3. Results and Discussion

3.1. Fresh concrete test results

The fresh properties test results of the investigated mixes are given in Table 3.

Table 3. Fresh properties test results.

Fiber Type	Mix ID	Slump flow		V-funnel		L-Box	Column Segregation
		D_{max}, mm	$t_{500\ mm}$, S	t_0, S	$t_{5\ min}$, S	H_2/H_1	S%
Without fibers	SCC-0	850	0.94	3.3	6.3	1	14.4
Polypropylene micro fibers (PM), 6 mm	SCC-PM 0.25	625	2	3.8	6.5	0.9	7.6
	SCC-PM 0.5	600	2.6	5	7	0.83	5
	SCC-PM 0.75	550	5	7	9.5	0.8	1
Polypropylene Long fibers (PL), 18 mm	SCC-PL 0.25	650	2.92	3.44	5.25	0.96	9.7
	SCC-PL 0.5	550	3	3.56	4.86	0.83	6.7
	SCC-PL 0.75	500	5.52	3.75	5.61	0.8	5.4
Polypropylene micro fiber mesh (PF), 6 mm	SCC-PF 0.25	750	1	3.41	4.87	0.96	5.6
	SCC-PF 0.5	625	1	3.91	5.26	0.93	4.5
	SCC-PF 0.75	600	1.26	4.68	5.89	0.88	2.5
Polypropylene long fiber mesh (PFL), 18 mm	SCC-PFL 0.25	650	2.5	4	6.48	0.96	9.1
	SCC-PFL 0.5	625	2.88	5.58	7.98	0.81	6.5
	SCC-PFL 0.75	580	4.85	6.79	8.15	0.8	5
Glass fibers (G), 18 mm	SCC-G 0.15	540	1.4	3.52	4.92	0.92	7.6
	SCC-G 0.25	500	2	4.8	6.1	0.85	5
	SCC-G 0.4	450	-	6.01	8.68	0.74	4.2
Steel fibers (S), 15 mm	SCC-S 0.5	850	1	3.73	3.91	1	9.4
	SCC-S 1	850	1.12	3.87	5.58	0.96	4.9
	SCC-S 2	800	1.15	4.22	6.19	0.93	1.4
Limits (EFNARC-05, and ESS 360-08)		600-800	2-5	6- 12	(t0+0) - (t0+3)	0.8-1	5-15 %

3.1.1. Slump flow test results

Slump flow test was carried out to ensure the horizontal free flow for the SCFRC. As seen in Table 3 the slump flow diameters D_{max} of all mixtures were in the range of 450-850 mm. Slump flow times $t_{500\ mm}$ were in the range of 0.94-5.52 S. The inclusion of fibers had a direct effect on the flow characteristics of SCC. The effect of different volume fractions and different aspect ratios of fiber on D_{max} is shown in Fig. 1.

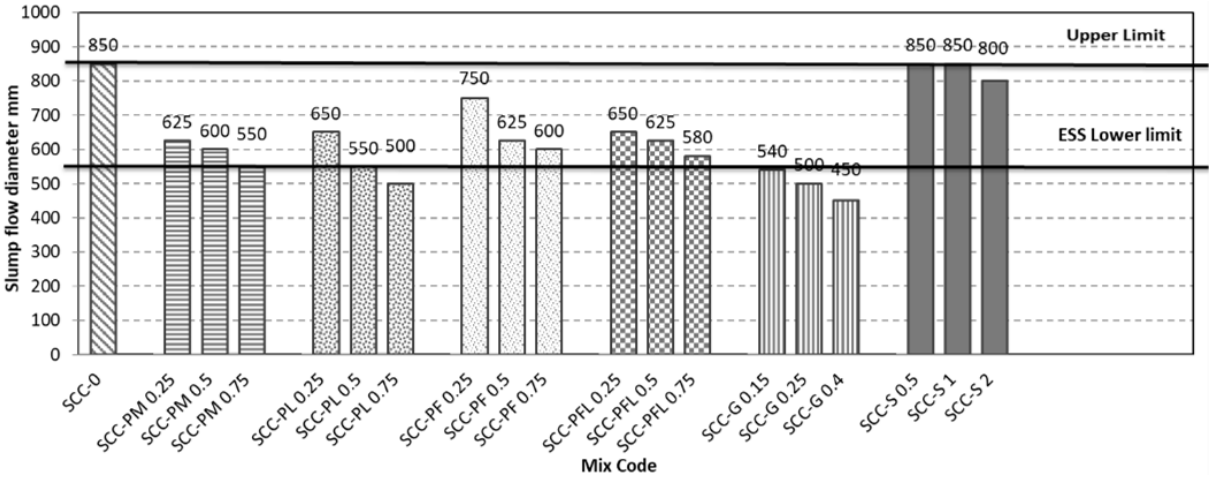

Fig. 1. Slump flow test results D_{max}.

3.1.2. L-Box test results

The L-box test is usually used to measure the filling and passing abilities. According to (EFNARC-05, and ESS 360-08) acceptance criteria for SCC, blocking ratio (H_2/H_1) should range from 0.8 to 1. The values of H_2/H_1 seem to be sensitive for G fibers addition. Whereas, H_2/H_1 seem to be less sensitive when PP and S fibers are added. Regardless of the fiber type, the increase in fiber volume fractions resulted in a drop in filling and passing abilities.

3.1.3. V-Funnel test results

The V-funnel test is usually used to assess the viscosity and filling ability of SCC. The test results are being the time periods taken for concrete to flow out of a V-shaped funnel just after filling the funnel and after 5 min (t_0, $t_{5\ min}$). The V-funnel test principal, apparatus, procedure and result computation are further described in (EFNARC-05, and ESS 360-07). Although increasing fiber volume fraction increased the t_0, but the difference between (t_0 - $t_{5\ min}$) ranged from 0.18 to 2.67 S that meets the requirements of (EFNARC-05, and ESS 360-08).

3.1.4. Column segregation test results

The column segregation test is usually used to evaluate the stability of SCC against segregation. The column segregation test principal, apparatus, procedure and result computation are further described in (ASTM C 1610-19). The test results are being the segregation percentage calculated from Eq. (3). SCC is generally considered to be acceptable if the percentage of segregation is less than 15% (ASTM C 1610-19).

$$S\% = 2\left[\frac{(Ct-Cb)}{(Ct+Cb)}\right]x100 \quad (3)$$

where: $S\%$ is the static segregation in percent, Ct is the mass of coarse aggregate in the top section of the column, and Cb is the mass of coarse aggregate in the bottom section of the column.

The column segregation test results proved that adding fibers to SCC mixes to produce SCFRC mixes enhanced stability of SCC against segregation that was observed based on column segregation test results. This could be attributed to the restriction of fibers to settlement of coarse aggregate particles. The reduction in segregation is up to 93% for mix with Polypropylene micro fibers in compared to control mix without fibers.

3.2. Hardened properties test results

The compressive strength, splitting strength as well as flexural strength test results at 7, 28 and 56-day age for the conducted mixes as a function of fiber types and fiber volume fractions are presented in Table 4.

3.2.1. Compressive strength

The effect of different volume fractions and different aspect ratios of fibers on the compressive strength (f_{cu}) are presented in Fig. 2. The f_{cu} test results show a tendency to be reduced compared with the control mix. This may be due to the excess of water to cementitious materials ratios that were slightly increased to achieve the flow ability requirements. Moreover, this is agreed with that for traditional fiber-reinforced concrete for which the f_{cu} is not considered a target for improvement (Apeh and Ameh, 2020).

Table 4. Hardened properties test results.

Mix ID	Compressive strength (MPa)			Splitting tensile strength (MPa)			Flexural strength (MPa)			G_f (N/m)	K_{1c} (N/m$^{2/3}$)	CMOD (mm)
	7	28	56	7	28	56	7	28	56			
SCC-0	48.5	65.9	78	3.11	3.7	4.23	9.27	9.77	10.96	44.33	6.35	0.035
SCC-PM0.25	30	37.7	53.9	3.01	3.59	4.21	9.34	9.86	11.08	36.93	7.87	0.037
SCC-PM0.5	40.5	50	58.3	3.12	3.75	4.44	10.42	12.03	13.03	48.78	8.45	0.041
SCC-PM0.75	44.8	52.5	73	3.35	4.07	4.45	10.58	12.42	13.53	50.27	8.91	0.045
SCC-PL0.25	29.3	35	42	3	3.6	4.29	9.74	11.97	12.53	197.08	7.49	0.039
SCC-PL0.5	39.2	44.6	54.4	3.24	3.86	4.69	9.78	12.6	13.35	202.76	7.58	0.044
SCC-PL0.75	43.6	50.2	61	3.7	4.8	5.12	10.3	13.04	13.95	219	7.7	0.047
SCC-PF0.25	41	53.4	55.8	3.06	3.64	4.23	9.49	10.13	11.46	81	8.15	0.038
SCC-PF0.5	45	56	60	3.13	3.8	4.48	10.75	11.65	13.73	132.69	8.22	0.042
SCC-PF0.75	46.4	61	66.8	3.49	4.08	4.49	11.84	13.45	13.96	168.72	8.4	0.046
SCC-PFL0.25	39	54	61	3.13	3.71	4.74	9.62	11.43	11.93	120.87	5	0.045
SCC-PFL0.5	44.6	56.1	67.2	3.5	4.31	4.89	10.1	12.8	13.81	164.15	7.04	0.05
SCC-PFL0.75	48.3	62	71	3.9	4.96	5.36	10.43	13.77	14.2	175.07	10.43	0.065
SCC-G0.15	35.1	42.4	47	2.95	3.42	3.91	9.3	9.89	10.97	19.47	5.71	0.037
SCC-G0.25	42.9	50	57.5	3.12	3.82	4.1	9.68	9.99	11.3	21.45	7.12	0.04
SCC-G0.4	49	60	67.9	3.14	3.96	4.45	10.03	10.32	11.32	32.58	8	0.045
SCC-S0.5	40	49.6	66.3	4.21	4.79	5.53	11.1	12.1	14.23	346.33	8	0.051
SCC-S1	45	55	72.2	4.4	5.9	6.02	11.5	14.07	15.18	920.52	8.41	0.067
SCC-S2	55	64.5	84	5.58	6.83	6.97	12.1	14.94	15.95	1237.68	13	0.094

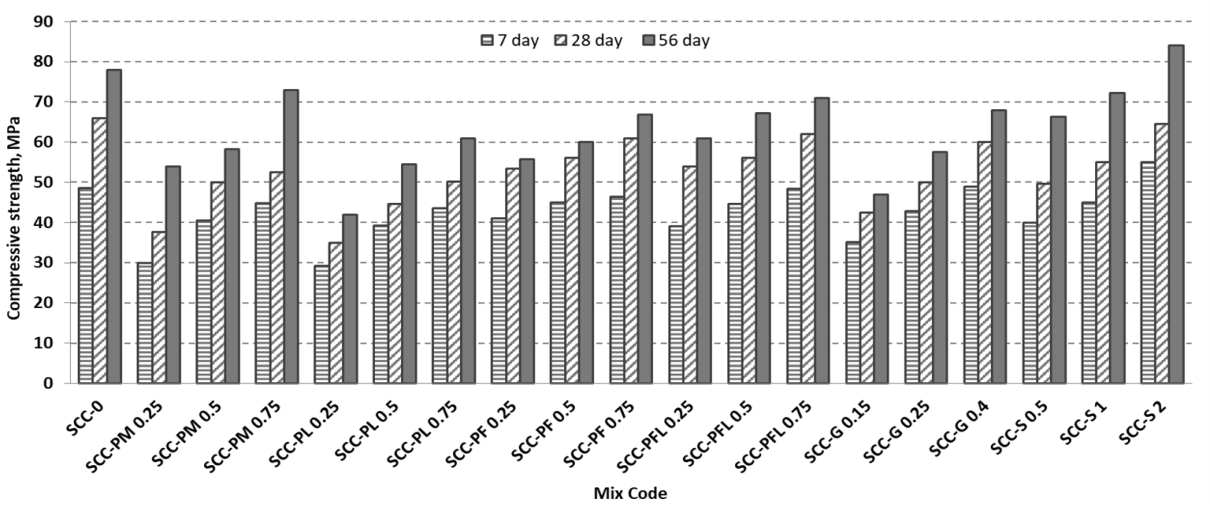

Fig. 2. Compressive strength test results.

3.2.2. Splitting tensile strength

The effect of different volume fractions and different aspect ratios of fibers on the splitting tensile strength (f_{sp}) are presented in Fig. 3. Mixes cast with the same type of fibers showed remarkable enhancements in the splitting tensile strength with ages. The maximum enhancements were 34%, 7% and 84.6%, for mixes incorporating PP, G and S fibers, respectively at 28-day compared to control mix SCC-0. The test results of f_{sp} indicated that the relativity higher efficiency of incorporating S fibers to enhance the f_{sp} compared with G and PP fibers.

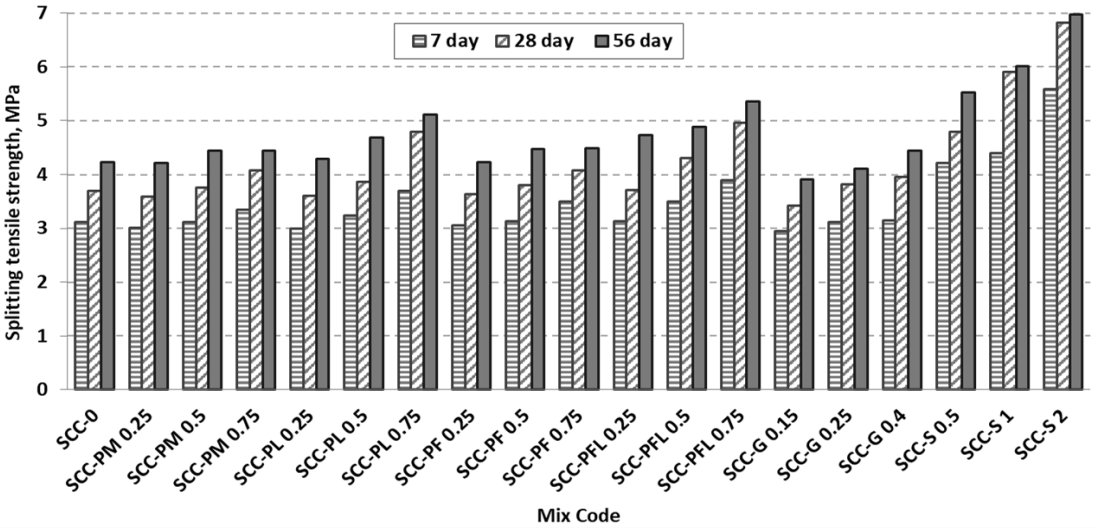

Fig. 3. Splitting tensile strength test results.

3.2.3. Flexural strength

The effect of different volume fractions and different aspect ratios of fiber on the flexural strength (f_f) are presented in Fig. 4. However, mixes cast with the same type of fibers showed remarkable enhancements in the f_f with ages. The maximum enhancements were 40.9%, 5.6% and 52.9% for mixes incorporating PP, G and S fibers, respectively at 28-day compared to control mix SCC-0.

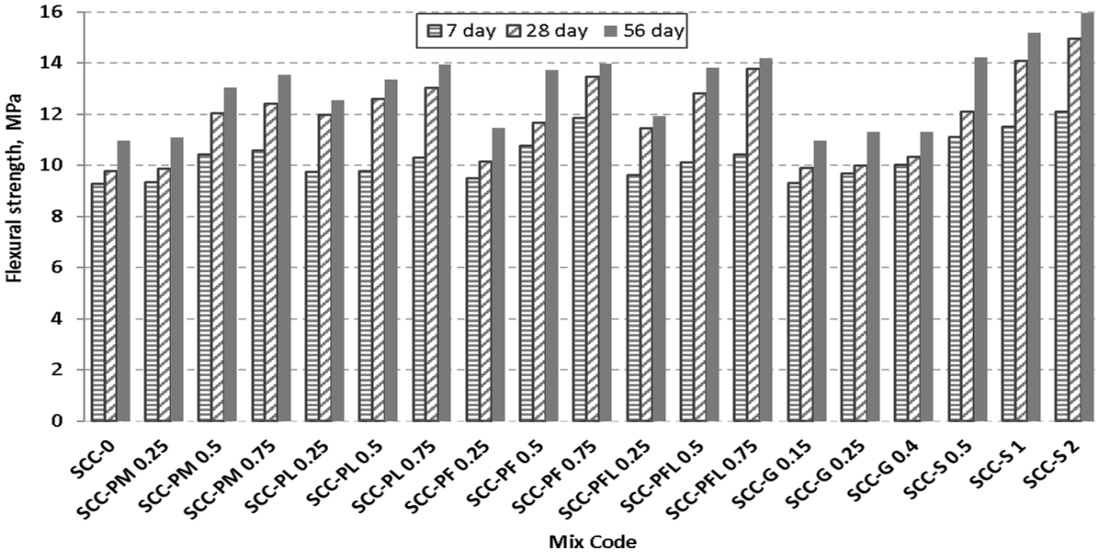

Fig. 4. Flexural strength test results.

3.3. Fracture properties test results

Fracture energy (G_f), fracture toughness (K_{1c}) and crack mouth opening displacement (CMOD) of the SCFRC were measured. The values of fracture properties are shown in Table 4.

3.3.1. Stress-deflection relationships

As the applied load on the notched beam increased, no cracks were observed until the load reached its peak value. A crack appeared at the end of the notch and started to propagate fast in the ligament when the load reached its peak value. The crack opened faster in the SCC specimens than in the SCFRC specimens. Failure occurred by opening of a single crack in the ligament in both types of concrete specimens. The stress deflection relationships of SCC and SCFRC specimens are given in Figs. 5 and 6. It is seen from these figures that the flexural stress increases with the increase of fiber volume fractions for all fiber types generally.

The post-peak parts of the stress–deflection curve "softening curves" seemed to be less steep with the increase of fiber volume fractions. The descending part of the stress–deflection curve, dropped faster in the SCC-0 specimen compared to that for the other SCFRC specimens.

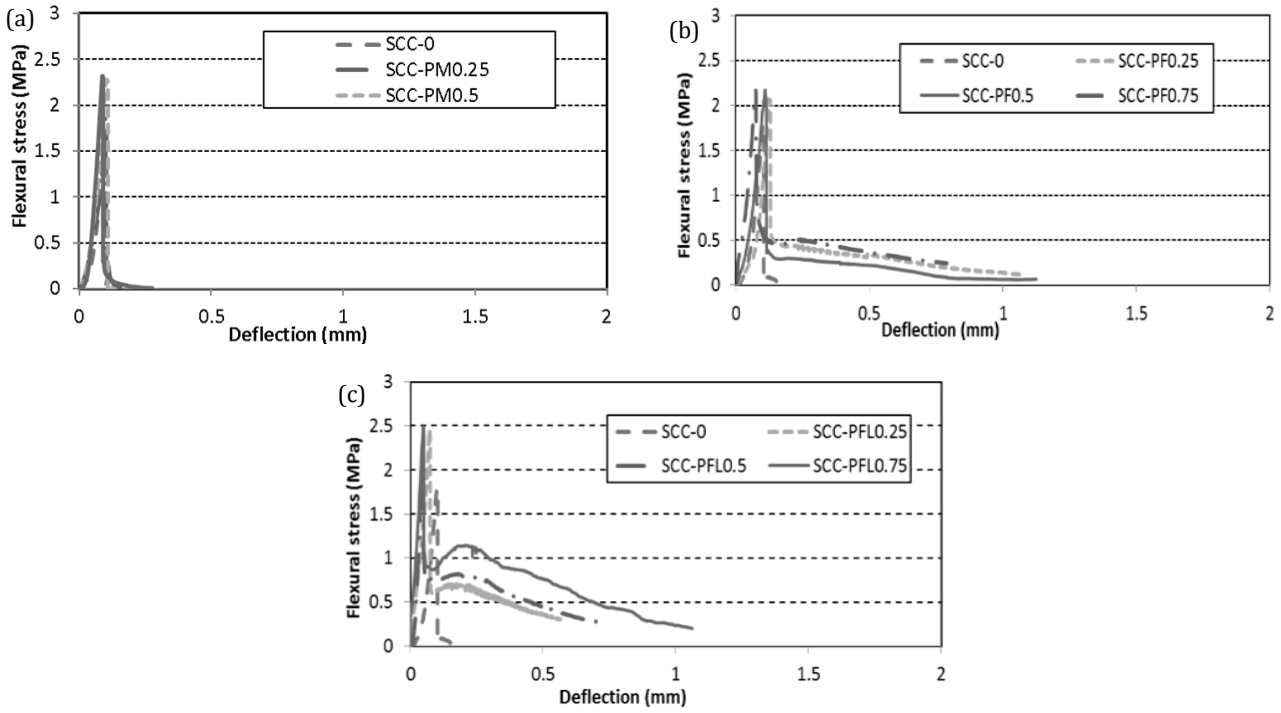

Fig. 5. Flexural stress vs deflection for notched specimens with polypropylene fibers: a) PP short fiber mesh; b) PP short fiber mesh; c) PP long fiber mesh.

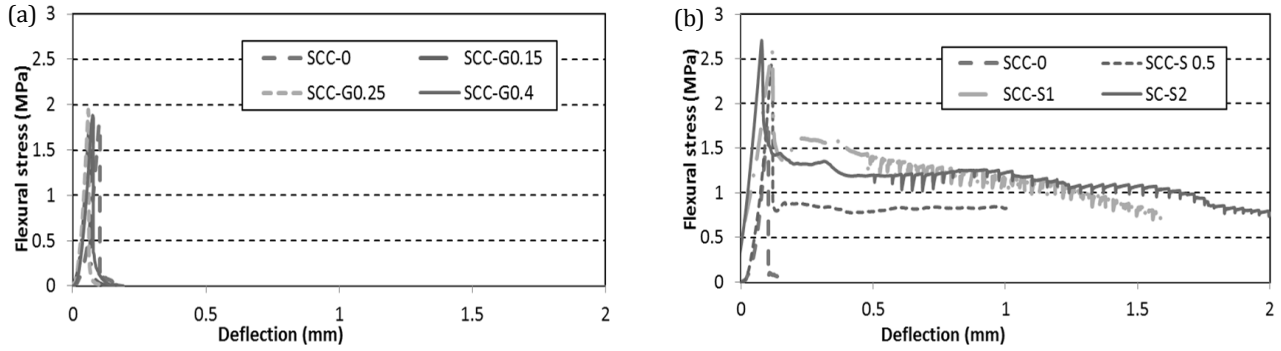

Fig. 6. Flexural stress vs deflection for notched specimens with fibers: a) Glass; b) Steel.

3.3.2. Effect of fiber types and volume fractions on fracture energy

The inclusion of fibers had a direct effect on the G_f of SCC. The effect of different types and volume fractions of fiber on G_f is plotted in Fig. 7. For mixes incorporating PP fibers, the G_f tends to increase with the volume fraction in all types of PP fibers. Increase the volume fraction of fiber from 0% to 0.75% increased the G_f, the maximum percentage increases were 13%, 394%, 279% and 295% for SCC-PM0.75, SCC-PL0.75, SCC-PF0.75 and SCC-PFL0.75, respectively compared to the control mix SCC-0. Whereas, the inclusion of G fibers did not improve the G_f of SCC but on the contrary had a slightly negative effect. This may be due to the relatively higher w/cm ratio used to maintain the SCC requirements. On the other hand, mixes containing S fibers showed a massive effect on the fracture energy of SCC, the. Increase the volume fraction of fiber from 0% to 2% increased the G_f. The maximum increases were 6.81, 19.67 and 26.92 times for SCC-S0.5, SCC-S1 and SCC-S2, respectively over the control mix SCC-0.

3.3.3. Effect of fiber type and volume fraction on fracture toughness

The effect of different types and volume fractions of fiber on the K_{1c} is plotted in Fig. 8. For mixes incorporating PP fibers, the K_{1c} tends to increase with the volume fraction, increases the volume fraction of fiber from 0% to 0.75% improved the K_{1c}, the maximum percentage enhancements were 40%, 21%, 32% and 64% for SCC-PM0.75, SCC-PL0.75, SCC-PF0.75 and SCC-PFL0.75, respectively compared to SCC-0. Whereas, the inclusion of G fibers slightly improves the K_{1c} of SCC, in case of SCC-G0.15 the percentage increase is not enough to reach the K_{1c} of SCC-0 and the increases were 12% and 25% for SCC-G0.25 and SCC-G 0.4, respectively, compared to SCC-0. On the other hand, for S fibers the maximum increases were 24%, 32% and 104% for SCC-S0.5, SCC-S1 and SCC-S2, respectively over to the control mix SCC-0.

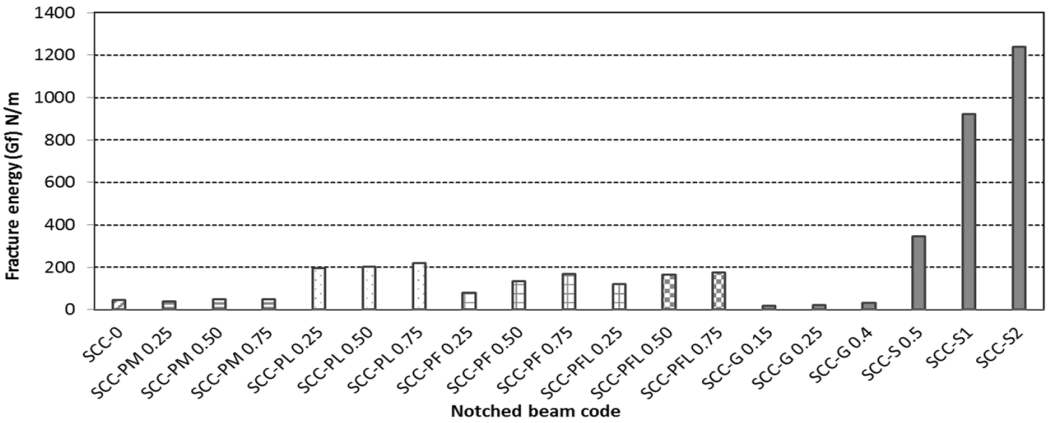

Fig. 7. Effect of fiber types and volume fractions on G_f.

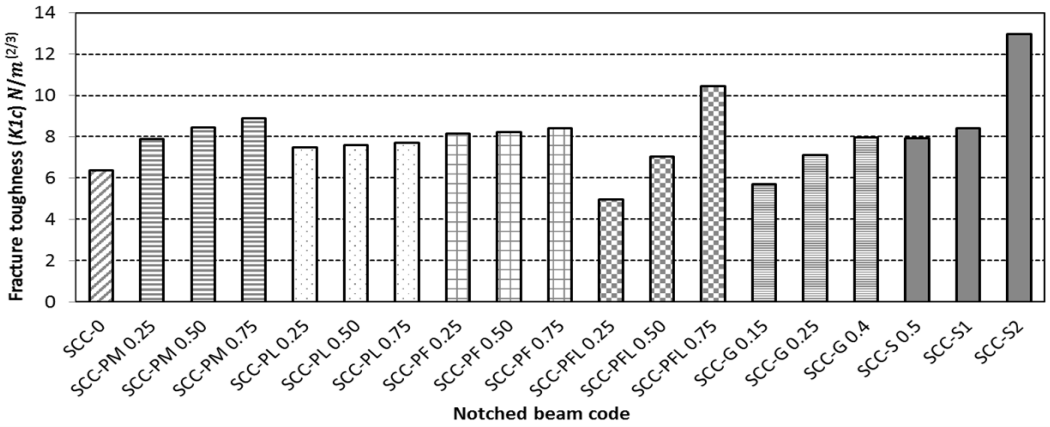

Fig. 8. Effect of fiber types and volume fractions on K_{1c}.

3.3.4. Effect of fiber types and volume fractions on crack mouth opening displacement

Results of CMOD for the investigated mixes are shown in Fig. 9. The CMOD is ranged from 0.035 mm to 0.067 mm. Regardless the fiber types, increasing the volume fraction of fibers increased the CMOD. For mixes containing PP fibers, the increases were 28.5%, 34.2%, 31.4% and 85.7% for SCC-PM0.75, SCC-PL0.75, SCC-PF0.75 and SCC-PFL0.75, respectively compared to SCC-0. Whereas, the increases for mixes incorporating G fibers were 5.7%, 14.2% and 28.5% for SCC-G0.15, SCC-G0.25 and SCC-G0.4, respectively compared to SCC-0. On the other hand, the increases for mixes incorporating S fibers were 45.7%, 91.4% and 168.5% for SCC-S0.5, SCC-S1 and SCC-S2, respectively compared to control mix SCC-0.

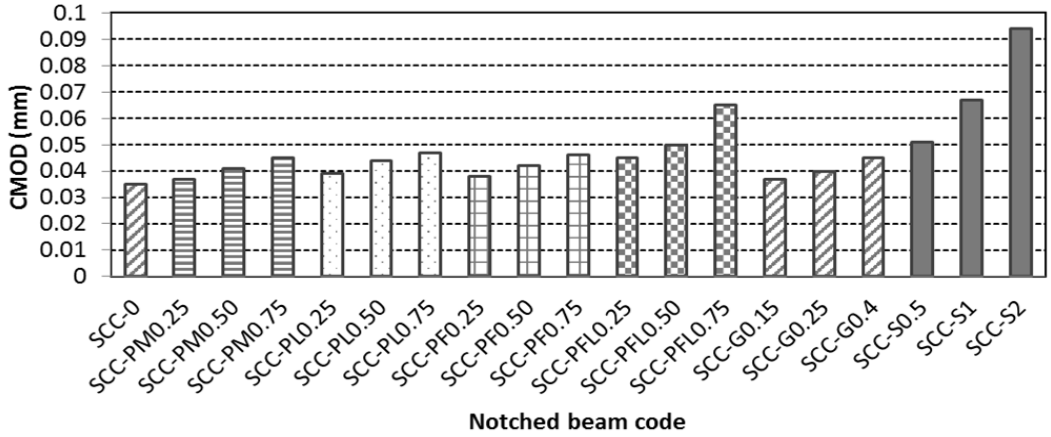

Fig. 9. Effect of fiber types and volume fractions on CMOD.

4. Conclusions

Based on the work performed in this study and the analysis conducted, the following conclusions could be drawn:

- Adding fibers to SCC mixes to produce SCFRC mixes enhanced stability of SCC against segregation that was observed based on column segregation test results. This could be attributed to the restriction of fibers to settlement of coarse aggregate particles. The reduction in column segregation test results was up to 93% with respect to control mix.
- In term of strength properties, concrete mixes incorporating steel fibers achieved higher compressive strength than polypropylene and glass fibers. The increase in compressive strength was up to 7.7% at 2% steel fibers compared to control mix without fibers at 56 days age. Whereas, the increases were remarkable in splitting tensile and flexural strengths, the increases were 84.6% and 52.9%, respectively at 28 days age.
- The efficiency of the conducted fibers in strength properties can be arranged in an ascending order at steel, polypropylene, and glass fibers, respectively.
- The inclusion of steel fibers had massive effect on the fracture energy of SCFRC. Using of 2% steel fibers enhanced G_f, by 26.9 times. Whereas, the maximum enhancement was 3.94 times over the control mix without fibers when 0.75% polypropylene fibers volume fraction was added.
- For the conducted fibers, using of 0.75% of polypropylene fibers enhanced the K_{1c} by 40%, 21%, 32% and 64% for mixes with polypropylene micro fibers, polypropylene Long fibers, polypropylene micro fiber mesh and polypropylene long fiber mesh, respectively. Whereas, only 25% enhancement was recorded when 0.4% glass fibers volume fraction was used. On the other hand, adding 2% steel fibers increased K_{1c} by 104%.
- Regardless of the fibers type, the increase in fiber volume fraction increased the CMOD. The increases were 28.5%, 34.2%, 31.4% and 85.7% for mixes with polypropylene micro fibers, polypropylene Long fibers, polypropylene micro fiber mesh and polypropylene long fiber mesh, respectively, when 0.75% polypropylene fibers volume fraction was added. Whereas, the increase was 28.5% when 0.4% glass fibers volume fraction was added. On the other hand, adding 2% steel fibers volume fraction increased CMOD by 168.5%.

Acknowledgements

The authors would like to express thanks are to staff of the Laboratory of Properties of Materials, Tanta University, Tanta, Egypt for their supports.

References

Adhikary SK, Rudzionis Z, Balakrishnan A, Jayakumar V (2019). Investigation on the mechanical properties and post-cracking behavior of polyolefin fiber reinforced concrete. *Fibers*, 7(1), 1–8.

Akcay B, Tasdemir M (2012). Mechanical behavior and fiber dispersion of hybrid steel fiber reinforced self-compacting concrete. *Construction and Building Materials*, 28, 287–293.

Alberti M, Enfedaque A, Gálvez J (2014a). On the mechanical properties and fracture behavior of polyolefin fiber-reinforced self-compacting concrete. *Construction and Building Materials*, 55, 274–288.

Alberti MG, Enfedaque A, Gálvez JC (2014b). On the mechanical properties and fracture behavior of polyolefin. *Construction and Building Materials*, 55, 274–288.

Apeh JA, Ameh JE (2020). Properties of steel fiber self-compacting concrete incorporating quarry dust fine powder. *Challenge Journal of Concrete Research Letters*, 11(1), 1–10.

Barros JAO, Figueiras JA (1999). Flexural behavior of steel fiber reinforced concrete testing and modeling. *Journal of Materials in Civil Engineering ASCE*, 11(4), 331–339.

Bazant Z, Pfeiffer P (1987). Determination of fracture energy from size effect and brittleness number. *ACI Material Journal*, 84, 463–480.

Biswajit J, Mohanty B (2015). Study on the mechanical properties and fracture behavior of chopped steel fiber reinforced self-compacting concrete. *International Journal of Engineering Research and Technology IJERT*, 4, 164–170.

Douglas R (2004). Properties of Self-Consolidating Concrete Containing Type Fly Ash with a Verification of the Minimum Paste Volume Method. *MSc. thesis*, Northwestern University, USA.

Elices M, Planas J (1996). Fracture mechanics parameters of concrete an overview. *Advanced Cement Based Materials*, 4, 116–127.

Ghazy MF, Abd Elaty MA, Dabaon O (2015). Rheological and mechanical characterization of fiber-reinforced self-compacting concrete. *1st International Conference on Advanced Structure and Geotechnical Engineering*, Hurghada, Egypt.

Groth P, Nemegeer D (1999). The use of steel fibers in self-compacting concrete. *Proceedings of the 1st International RILEM Symposium on Self-Compacting Concrete*, Sweden, 497–507.

Hoang AL, Fehling E (2017). Influence of steel fiber content and aspect ratio on the uniaxial tensile and compressive behavior of ultra high performance concrete. *Construction and Building Materials*, 153, 790–806.

Hordijk DA (1991). Local Approach to Fatigue of Concrete. *PhD Thesis*, Delft University of Technology, Netherlands.

Khayat K, Roussel Y (1999). Testing and performance of fiber-reinforced self-consolidating concrete. *Proceedings of the 1st International RILEM Symposium on Self-Compacting Concrete*, Sweden, 509–521.

Kytinou VK, Chalioris CE, Karayannis CG (2020). Analysis of residual flexural stiffness of steel fiber reinforced concrete beams with steel reinforcement. *Materials*, 13, 1–24.

Morelli F, Amico C, Salvatore W, Squeglia N, Stacul S (2017). Influence of tension stiffening on the flexural stiffness of reinforced concrete circular sections. *Materials*, 10, 669.

Okamura H, Ozawa K (1995). Mix design for self-compacting concrete. *Concrete Library of JSCE*, 25, 107–120.

Persson B (2001). A comparison between mechanical properties of self-compacting concrete and the corresponding properties of normal concrete. *Cement and Concrete Research*, 31, 193–198.

Sabir B, Wild S, Asili M (1997). On the tortuosity of the fracture surface in concrete. *Cement and Concrete Research*, 27, 785–795.

Smarzewski P, Barnat-Hunek D (2015). Fracture properties of plain and steel polypropylene fibers, *Materials and Technologies*, 49, 563–571.

Wittmann FH (2002). Crack formation and fracture energy of normal and high strength concrete. *Sadhana*, 27, 413–423.